20

Optical clearing of human skin *in vivo* using aqueous solutions of sorbitol, xylose, and DMSO

© K.V. Berezin¹, E.Yu. Stepanovich², A.M. Likhter², K.N. Dvoretsky^{3,¶}, E.V. Grabarchuk², E.A. Genina^{1,4}, I.Yu. Yanina^{1,4}, A.B. Pravdin¹, Yu.I. Surkov¹, V.V. Tuchin^{1,4,5}

- ¹ Saratov National Research State University, Saratov, Russia
- ² Astrakhan State University, Astrakhan, Russia
- ³ Saratov State Medical University, Saratov, Russia
- ⁴ Tomsk State University, Tomsk, Russia
- ⁵ Institute of Precision Mechanics and Control, FRC "Saratov Scientific Centre of the RAS", Saratov, Russia

Received February 06, 2025 Revised March 04, 2025 Accepted April 07, 2025

Using the method of optical coherence tomography (OCT), results of immersion optical clearing of human skin *in vivo* were obtained using aqueous solutions of sorbitol, xylitol, D-xylose, and dimethyl sulfoxide (DMSO) as immersion agents. To assess the effectiveness of optical clearing, the rate of change in the scattering coefficient was determined using the averaged A-scan of the OCT signal in the dermis region at a depth of 350 to $700\,\mu\text{m}$. As a result of molecular modeling using classical molecular dynamics methods (GROMACS), the number of hydrogen bonds formed per unit time for each agent was determined, as well as the influence of these agents on the spatial volume of the collagen peptide ((GPH)₃)₉. Quantum chemistry methods HF/STO3G/DFT/B3LYP/6-311G(d) were used to calculate the intermolecular interaction energy of immersion agent complexes with a fragment of the collagen peptide ((GPH)₃)₂, and correlations were established between the effectiveness of optical clearing and the intermolecular interaction energy. Non-classical hydrogen bonds formed during the interaction of DMSO with the collagen peptide and water molecules are discussed in detail. The effective diffusion coefficient of DMSO in rat skin ex vivo was calculated, with an average value of $(4.1 \pm 3.1) \times 10^{-6}$ cm²/sec.

Keywords: molecular modeling, optical clearing of human skin, hydrogen bonds, molecular dynamics, quantum chemistry, immersion agents, diffusion coefficient.

DOI: 10.61011/EOS.2025.05.61654.35-25

Introduction

The use of modern methods of photomedicine and biomedical optics for the diagnosis and therapy of diseases is fraught with problems that arise due to the fact that the skin and most other biological tissues have strong scattering of light in the visible and near-infrared regions. This scattering occurs due to randomly oriented inhomogeneities of refractive indices at the boundaries of various macromolecular structures, mainly on collagen fibers, which are mainly responsible for light scattering in the skin [1].

In particular, these problems are overcome by introducing biocompatible molecular agents into the tissue, which contribute to its optical clearing (OC) to one degree or another [1–6]. Quite a lot of generalizing studies such as analytical reviews and monographs [1–11] have been devoted to experimental *in vivo*, *ex vivo* and *in vitro* implementations of the OC method on various types of biological tissues, which indicates the relevance of the problem. Many papers describe interesting applications of the method or prove its versatility and multimodality. For example, the use of the method in criminology for postmortem imaging of the perinatal dura mater and superior sagittal sinus using optical coherence tomography

(OCT) is described in Ref. [12]. The synergistic effect of an immersion agent (PEG-400), two chemical permeability enhancers of biological tissue (triazine and 1,2-propanediol) and mechanical massage on the effectiveness of OC of rat skin was evaluated in vivo by OCT methods in Ref. [13]. Dimethyl sulfoxide (DMSO) is often used as bio-tissue permeability enhancer [14-17]. It is also used as an optical clearing agent (OCA) [18,19]. A mathematical model was proposed in Ref. [20] to solve the inverse problem of radiation transfer in biological tissues in order to determine the scattering and absorption coefficients for OC, taking into account the osmotic activity of OCA. Two approaches for noninvasive investigation of local diffusion of immersion OCA using optical coherence tomography (OCT) are described in Ref. [21]. The effect of model diabetes mellitus on OC of the skin of laboratory mice was considered in Ref. [22] and a significant difficulty in the diffusion of OCA in glycated tissues was shown. The mechanism of skin OCA was studied in Ref. [23] using glycerin and the radiopaque drug Omnipaque® (yogexol) as OCA by imaging using autofluorescence with two-photon excitation and second optical harmonic (SHG-imaging). The paper in Ref. [24] is devoted to elucidating the mechanisms of collagen tissue formation in normal conditions and during

[¶]e-mail: dcn@yandex.ru

glycation using multiphoton tomography. The results of studies of the dehydrating properties of OCA are presented in Ref. [25] and it is noted that dehydration is only one of the possible mechanisms leading to OC of biological tissues. Another mechanism for reducing the scattering cross-section of collagen fibers may be their reversible dissociation, which is also directly related to the molecular interaction of OCA and collagen [26]. Recently, a new approach has been proposed in Ref. [27] to achieve optical transparency in biological tissues, which uses highly lightabsorbing substances to change the refractive index of the aquatic environment. This leads to a significant reduction in light scattering. The study showed that food-grade watersoluble dyes such as tartrazine can make tissues transparent in the red and near-infrared regions of the spectrum. This method is based on increasing the actual refractive index of an aqueous biological medium (blood plasma, interstitial fluid, or cytoplasm) due to the phenomenon of abnormal dispersion and was proposed and studied in detail in the works of hboxjcite28-32, where hemoglobin was used as an absorbing substance.

Studies in the field of the interaction of OCA with biological tissues opens the way to understanding the physical and biophysical processes underlying OC at the molecular level [3,6,26,33–37]. This, in turn, will make it possible to find new effective OCA with specified properties that are optimal for a specific type of biological tissue.

The present work is a continuation of the authors' study of the molecular mechanisms of OC of biological tissues [6,26,33-37] using the example of the action of four OCA of two polyatomic alcohols (sorbitol, xylitol), xylose monosaccharide and DMSO. Molecular modeling was previously performed for the synthesis of sorbitol and xylitol and a correlation was established between the energy of intermolecular interaction and the optical clearing efficiency (OCE) based on experimental ex vivo data on human and rat skin [4]. We obtained in vivo experimental data on OCE of human skin in this study and checked the correlation with them. In addition, starting with the study in Ref. [32], the protocol of molecular modeling based on the semiempirical PM6 method was replaced by the nonempirical HF (Hartree-Fock) [38], since a preliminary study found that the semiempirical method gives incorrect results for molecules with complex electronic structure, such as yogexol.

Experimental methods and results

Skin OC *in vivo* was performed using 70% aqueous sorbitol solution, 38% xylitol solution, 50% D-xylose solution and 100% DMSO.

OCA solutions were prepared by precise weighing: the components of the solution were weighed on microanalytical scales (hboxDA-225DC with calibration (0.001 g), Bel Engineering, Italy), which were then transferred to a

measuring flask for dissolution and thoroughly mixed using a vortex agitator.

Refractive indices were measured using an Abbe Atago DR-M2 1550 multi-wavelength refractometer (Atago, Japan) at 589 and 930 nm wavelengths at a temperature of 24.0,°C. The values of the refractive indices, molecular weights, and osmolality of the OCA solutions are given in Table 1.

The OCT method was used to evaluate the optical clearing properties of the selected agents. In this work, a spectral OCT GAN930V2-BU (Thorlabs, USA) with a central radiation wavelength of $930 \pm 5\,\mathrm{nm}$ was used; the longitudinal resolution in air is $6.2\,\mu\mathrm{m}$, and the transverse resolution is $\sim 9.6\,\mu\mathrm{m}$; the size of the cross-scan area is $2\,\mathrm{mm}$

The study was conducted in accordance with the Helsinki Declaration and was approved by the Ethics Committee of Saratov State Medical University named after V.I. Razumovsky (№ 11 dated August 7, 2022). The measurements were performed on the back of the forearm. Previously, the stratum corneum on this area of the skin was removed using medical tape. Two-dimensional scans (B-scans) of the study area were recorded for 60 minutes with an interval of 3 minutes. Five volunteers between the ages of 27 and 56, of both sexes, participated in these measurements. A total of five measurements were made for each immersion agent.

The recorded OCT signal, according to the single scattering model [22,40–43], is described by the expression

$$R(z) \sim \exp(-\mu_t z),$$
 (1)

where the attenuation coefficient

$$\mu_t = \mu_s + \mu_s, \tag{2}$$

z is the scan depth.

Since the absorption coefficient μ_a of the skin is significantly less than the scattering coefficient μ_s in the range of 930 \pm 100 nm [1], the absorption coefficient μ_a can be neglected, so R(z) can be approximated by the following expression [44]:

$$R(z) = A \exp(-\mu_s z) + B, \tag{3}$$

where A is the proportionality coefficient equal to $P_0a(z)$, P_0 is the power of optical radiation incident on the skin surface, a(z) is the local back reflectance, which characterizes the skin's ability to scatter light back and is determined by a local jump (fluctuation) in the refractive index, B is the background signal. The selection of coefficients in the above expression for approximating the experimental curve makes it possible to estimate the scattering coefficient of the object of study averaged over the selected segment of the depth of the longitudinal scan z.

Fig. 1 shows OCT images (*B*-scan) of the skin immediately after applying an aqueous xylose solution to it, an averaged *A*-scan of the OCT signal of the dermal layer of human skin, as well as an approximating curve based on a

Immersion agent	Chemical formula	Molecular weight, g/mol	Refraction index $\lambda = 589 \text{nm}$	Refraction index $\lambda = 930 \text{nm}$	Osmolality, Osm/kg H ₂ O
Sorbitol aqueous solution (70%)	C ₆ H ₁₄ O ₆	182.17	1.4591	1.4515	15.2 [4]
Xylitol aqueous solution (38%)	$C_5H_{12}O_5$	152.15	1.3971	1.3897	15.6 [4]
D-Xylose aqueous solution (50%)	$C_5H_{10}O_5$	150.13	1.4169	1.4098	8.43 [39]
DMSO	C ₂ H ₆ OS	78.13	1.4768	1.4669	14.08*

Table 1. Physical properties of clearing agents

Note * Calculated value.

single scattering model (formula (3)). OCT signals in the form of A-scans were averaged over the entire scan width (2 mm) along the skin surface. The values of the scattering coefficient were determined in the area of the averaged A-scan at depths from 350 to $700\,\mu\text{m}$.

Visually, from 1, a, it can be seen that over time, the image of the upper layers of the skin becomes darker, while the deeper layers become slightly lighter, which indicates that under the influence of OCA, light scattering by the upper layers of the skin decreases, and light passes into the lower layers, where it is reflected more intensely from heterogeneities, which carries information about deep-lying objects inside the tissue. Quantitatively, this is well reflected in Fig. 1, b.

Numerical values of the scattering coefficient obtained using an averaged A- scan in the dermis area at depths from 350 to $700\,\mu\text{m}$, were used to evaluate the OCE of the skin *in vivo*. The dependence of the scattering coefficients under the action of the clearing agent on the observation time is shown in Fig. 2. It can be seen that for all agents used in the study, the value of the scattering coefficient μ_s over a long range of exposure times is well described by the linear regression model (the correlation coefficient R^2 is 89-97%).

The values of the modulus of the average rate of decrease in the scattering coefficient were used for a numerical estimation of the OCE of human skin. These values represent the slope value determined from the regression line equations (Table 2).

Molecular modeling

The structures of the collagen mimetic peptide $((GPH)_3)_9$ [45] and its abbreviated version $((GPH)_3)_2$ (Fig. 3) selected by us for modeling represent the largest part of the regular domains of human collagen. Their spatial structure was constructed according to the Protein Data Bank (PDB). Hydrogen atoms were also added to the models, followed by optimization of their geometric structure by the method of molecular mechanics [46]. The structure shown in Fig. 3, a has a structurally molecular pocket of the order of 10×15 Å, which contains four functional groups: two hydroxyl groups (O_1H_1, O_2H_2) and

two carbonyl (C_3O_3 , C_4O_4), which form hydrogen bonds with OCA molecules. Three of them are located on one chain, and the group O_1H_1 is located on the other chain.

The molecular modeling protocol consists of the following steps.

Construction and analysis of molecular structures of OCA

A conformational analysis of the molecular models of the considered OCA was performed at the initial step, using the DFT/B3LYP/6-311+G(d,p) [47,48] method implemented in the Gaussian program [49]. Their minimum energy spatial configurations were found (Fig. 3). The calculation of the oscillatory wave numbers (followed by their verification for negative values) was used to confirm the fact that all molecular models are at their local energy minima.

Fig. 3 shows that the conformations with the maximum number of intramolecular hydrogen bonds have the lowest energy among the molecules with hydroxyl groups. DMSO molecule has the simplest structure. It is symmetric and belongs to the symmetry group Cs. The parameters of the OCA molecular models calculated at this stage were further used in molecular dynamics and molecular docking.

Classical molecular dynamics

The intermolecular interaction of clearing agents with collagen peptides was simulated at this step using the GROMACS classical molecular dynamics package [50] with the force field AMBER-03 [51]. The model scene consisted of a three-dimensional cell (with dimensions $3 \times 3 \times 9 \text{ nm}$) with periodic boundaries. 20 molecules of the clearing agent were randomly distributed within the cell before each simulation began. The initial velocities of the atoms had a Maxwellian distribution and were set using a random number generator from the GROMACS package. During the simulation, the Berendsen thermostat and barostat [52] were used to ensure convergence of the thermodynamic parameters of the system to the following values: $T_0 = 300 \,\mathrm{K}$ and $P_0 = 1$ bar. The simulation time step was 0.0001 ps, and the total time was 100 ps. The system state was recorded every 0.1 ps. The recorded trajectories of molecular motion

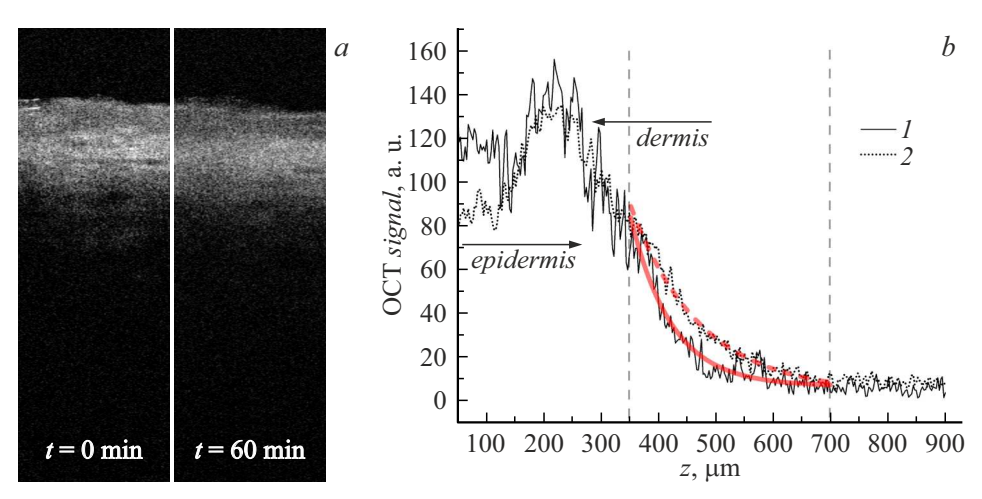


Figure 1. Measurements of the scattering coefficient μ_s in the dermis area after applying a xylose solution to the surface based on an analysis of the OCT signal distribution averaged over depth using a single scattering model. (a) Images of a B-scan of the skin in vivo, according to a fragment of which the OCT signal was averaged immediately after application and after 60 min exposure. (b) Depth distribution of the averaged OCT signals (thin curve) and the result of approximation according to the single scattering model (red curves): I — immediately after application of the aqueous solution of D-xylose, 2 — after 60 min of action of D-xylose. Dashed lines indicate the boundaries of the sections (from 350 to 700 μ m) where the value μ s was estimated. The arrows indicate the layers of the skin: epidermis and dermis.

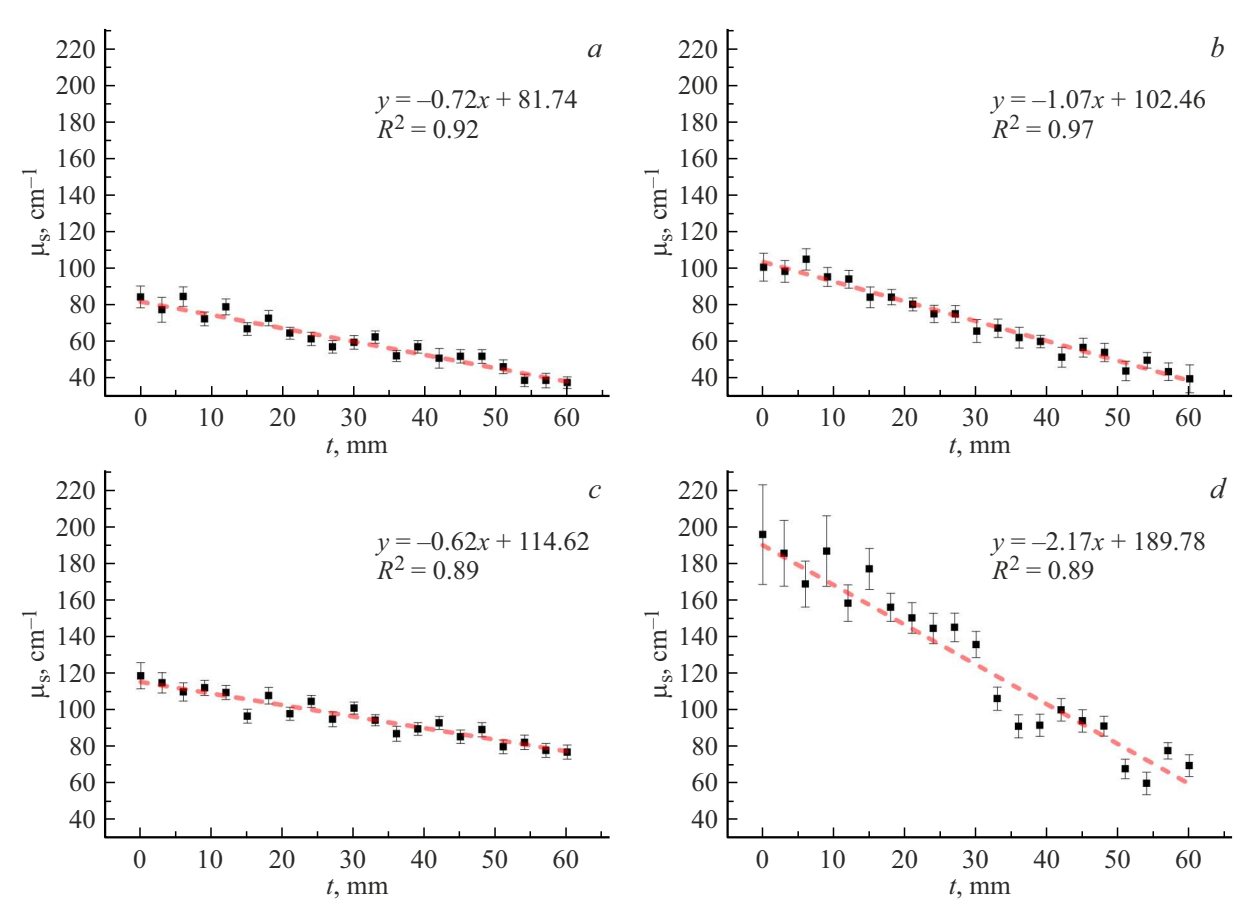


Figure 2. Time dependences of the scattering coefficient μ_s in the dermal area $(350 - 700 \, \mu\text{m})$ in vivo of human skin when exposed to the following clearing agents: xylitol (a), sorbitol (b), xylose (c) and DMSO (d). The linear approximation is marked with a dashed line and expressed as an equation.

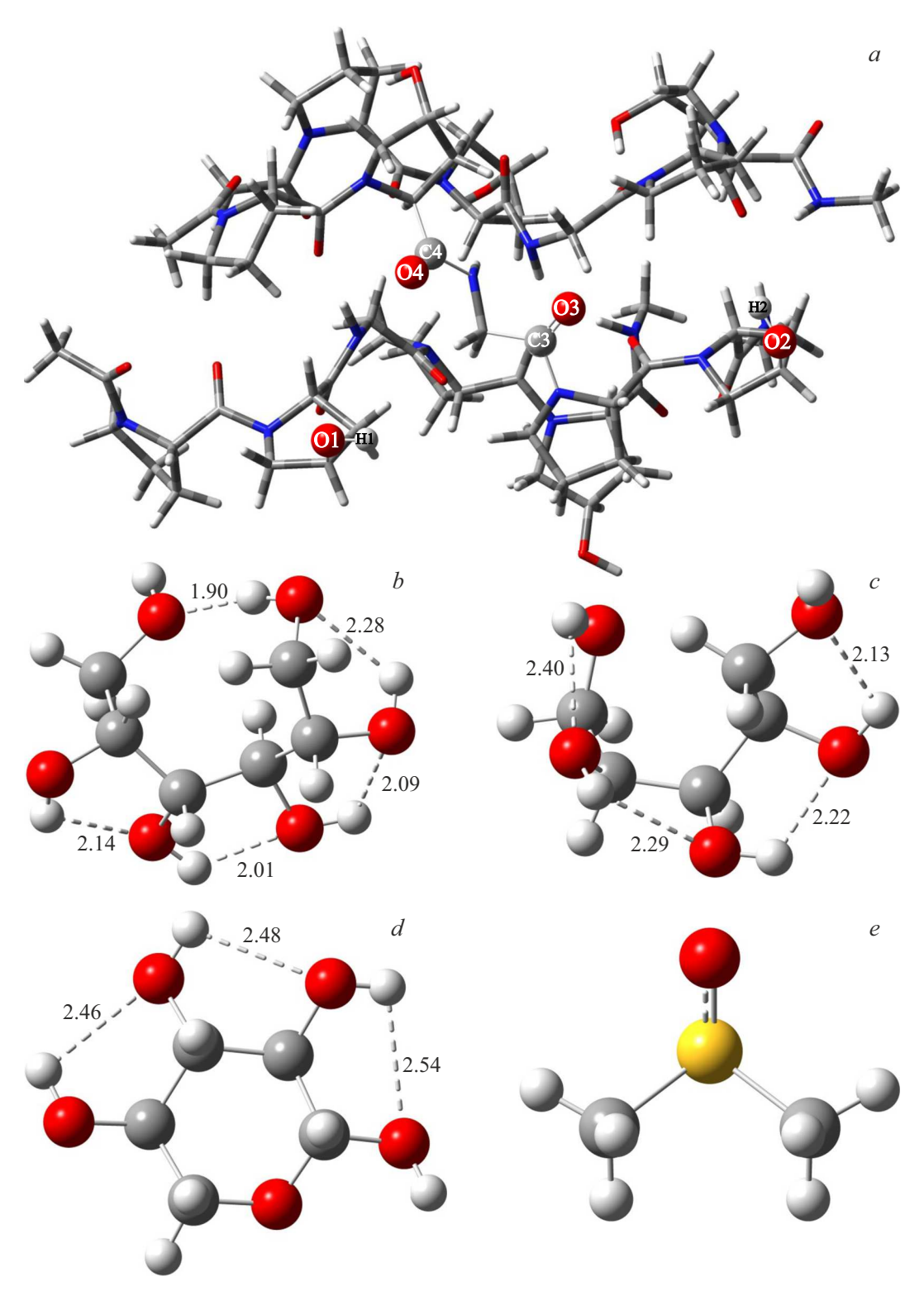


Figure 3. The structures of the shortened version of the peptide are collagen mimetics $((GPH)_3)_2$, optimized by HF/STO-3G (a), and the lowest energy spatial structures of sorbitol molecules (b), xylitol (c), D-xylose (d) and DMSO (e), calculated by the B3LYP/6-311G+(d,p) method. Letters with numbers indicate the atoms of functional groups with which hydrogen bonds are formed. The dashed lines show intramolecular hydrogen bonds between hydroxyl groups. The numbers in the figure show the lengths of hydrogen bonds in angstroms.

Nº	OCA	N, ps ⁻¹	ΔE , kJ/mol	OCE, cm ⁻¹ min ⁻¹	
1	Xylitol	0.968 ± 0.099 [50]	-131.1	0.72 ± 0.05	
2	Sorbitol	1.131 ± 0.096 [50]	-143.8	1.07 ± 0.04	
3	Xylose	0.960 ± 0.192	-114.8	0.62 ± 0.05	
4	DMSO	0.393 ± 0.104	-230.3 (-139.1)*	2.17 ± 0.12	

Table 2. The number of hydrogen bonds per unit time, the values of the intermolecular interaction energies (kJ/mol) between the collagen fragment $((GPH)_3)_2$ and the studied and compared clearing agents, calculated using the HF/STO-3G/B3LYP/6-311G method(d), as well as experimental OCE values and their errors in the form of a standard deviation

Note * Energy of interaction with one DMSO molecule.

were processed using the GROMACS package and the VMD (Visual Molecular Dynamics) program [53]. The simulation was performed 30 times for each studied system, followed by averaging of the results. An example of the intermolecular interaction of clearing agents with collagen peptides is shown in Fig. 4.

As part of this modeling stage, the average number of hydrogen bonds formed between clearing agents and collagen per unit time was estimated. It was assumed that a hydrogen bond is formed if the following geometric criteria are met: $R \leq 3.5 \, \text{Å} \, [54]$ and $\phi \leq 30 \, ^{\circ}$, where R is the distance between the donor atom A covalently bound to the hydrogen atom H, and the acceptor atom B of another molecule or functional group of the same molecule, ϕ is the angle formed by the bonds AH and AB.

Also, the change in protein volume is an informative parameter for establishing a correlation between the interaction of OCA with the protein collagen and OCE [55]. The time dependence of changes in the volume of collagen peptides under the action of OCA was studied within the framework of molecular modeling. A fragment of collagen microfibril $5((GPH)_{12})_3$ was selected as the structure of the collagen mimetic peptide for modeling. For this peptide, the model scene consisted of a cell with side sizes $5 \times 13 \times 5$ nm, in the center of which the collagen peptide was placed. The rest of the space was filled with an aqueous solution (Fig. 4, c, d). The modeling time step was chosen to be 0.0001 ps, and the total modeling time was 1 ps. The system status was recorded every picosecond.

At the next stage of modeling, using molecular docking (AutoDockVina [56] program), the structures of hydrogen-bound complexes "model of the collagen peptide and the considered OCA" were constructed (Fig. 3). Ten most energetically stable configurations of intermolecular complexes were selected for each OCA.

Methods of quantum chemistry

At this stage, structural optimization of all complexes of $((GPH)_3)_2$ -OCA obtained by molecular docking was carried out using the HF/STO3G method, followed by refinement of the electronic energy using a single SCF (Self-Consistent

Field) procedure using the B3LYP/6-311G(d) method. The total electronic energy of the collagen peptide $((GPH)_3)_2$ and all OCA were calculated using a similar procedure. Next, the energy of the intermolecular interaction was calculated using the formula

$$\Delta E = E_{\rm comp} - E_{\rm GPH} - E_{\rm OCA},\tag{4}$$

where E_{comp} is the total electronic energy of the complex $((GPH)_3)_2$ -OCA, E_{GPH} is the total electronic energy of the collagen peptide $((GPH)_3)_2$, E_{OCA} is the total electronic energy of this OCA. Fig. 5 shows intermolecular complexes $((GPH)_3)_2$ -OCA with maximum interaction energy.

Evaluation of effective diffusion constant and effective optical clearing

A method for estimating the diffusion constant of immersion fluids in tissues based on measuring the time dependence of collimated transmittance in tissue samples immersed in an OCA solution is described in detail in Ref. [21]. The theory of free diffusion was used for the calculation, taking into account the following approximations: 1) the exchange flow of the solution into the skin and water from it at a given point is proportional to the concentration gradient of the OCA at that point, 2) the diffusion coefficient is constant inside at all points of the studied sample. The collimated transmittance spectra of the skin were recorded in the wavelength range of 400–1000 nm using a USB4000 spectrometer (Ocean Optics, USA) every minute for an hour from the moment the sample was placed in a DMSO solution until the spectra stopped changing.

The time dependence of the coefficient of collimated transmittance of a skin sample has the form

$$T_c(t) = \exp(-\mu_t(t)l), \tag{5}$$

where μ_t is the attenuation coefficient, which is the sum of the scattering and absorption coefficients, l is the thickness of the sample.

The time interval over which the coefficient changes were observed was considered for estimating the OCE based on the kinetics of the attenuation coefficient in the studied spectral range: OCE $\approx (\mu(t=0) - \mu_t(t))/t$.

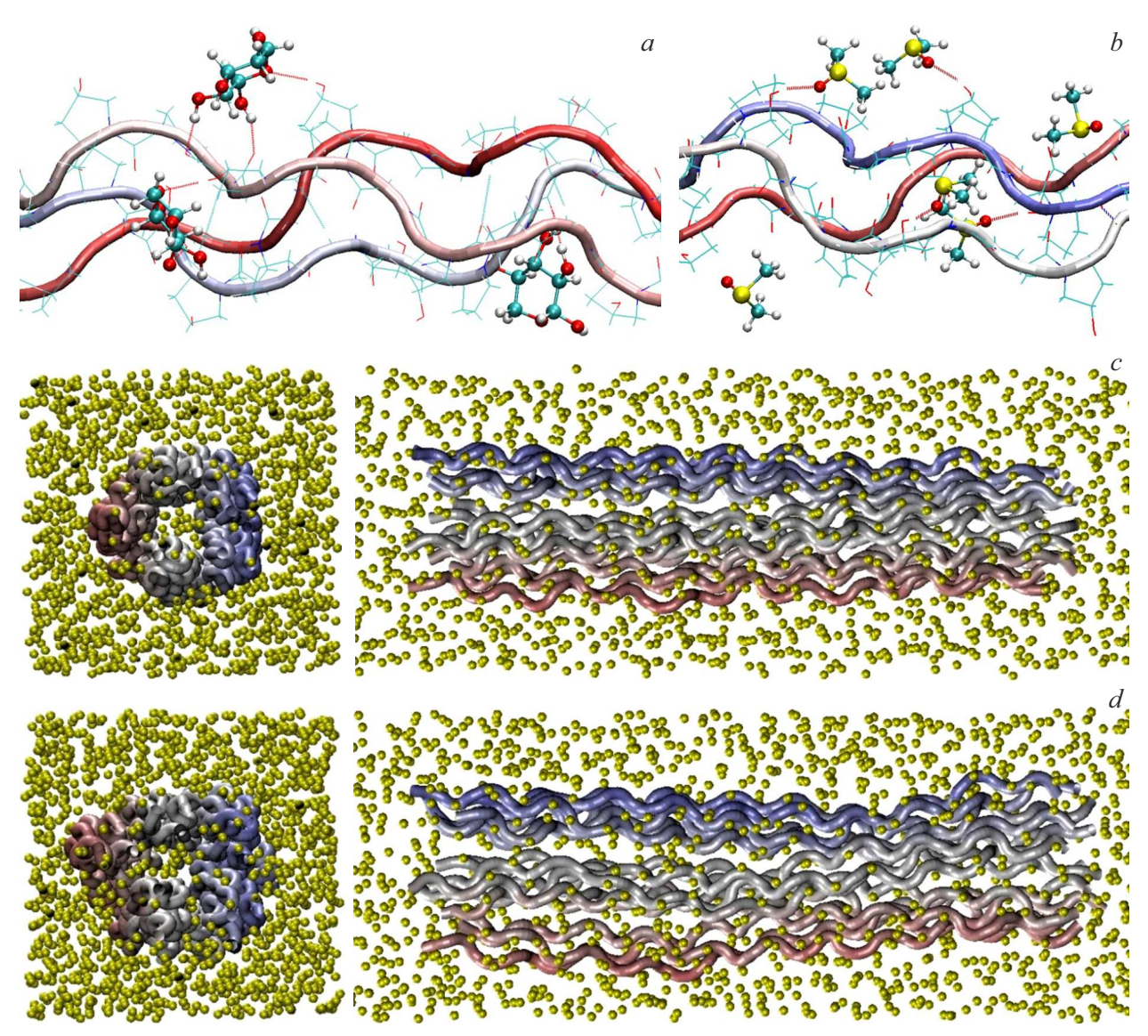


Figure 4. Fragments of spatial structures of the hydrogen-bound collagen peptide complex $((GPH)_3)_9$ with xylose molecules (a), DMSO (b) and spatial distribution of DMSO molecules around the collagen peptide $5(GPH_{12})_3$ at the beginning of observation (c) and after 1 ns (d) in two different projections obtained in the framework of classical molecular dynamics.

The objects of the study were 10 skin samples of white outbred rats obtained by autopsy, which were stored in saline solution at a temperature of $4-5\,^{\circ}\mathrm{C}$ for 24 h. The measurements were carried out at room temperature of $20\,^{\circ}$ C.

Discussion of the results

Experimental data (Fig. 2) show that DMSO has the best OCE among considered OCA, followed by sorbitol, xylitol and D-xylose in descending order. Molecular modeling performed using classical molecular dynamics shows that the correlation between parameters such as the number of hydrogen bonds per unit time and OCE exists only for highly conformationally mobile chain-type structures, which

include the unclosed alcohols glycerol, sorbitol, and xylitol (Fig. 6).

This is attributable to the fact that only the number of hydrogen bonds is taken into account. As our previous research shows [37], there is no direct relationship between the number of hydrogen bonds and the energy of complexation. Factors such as the difference in electronic structures, competition between intermolecular and intramolecular hydrogen bonds in the OCA, and the presence of conformationally mobile groups with hydroxyl or carbonyl groups must be taken into account here. They include hydroxymethyl groups in sugars. The number of functional groups on the ring side that the molecule interacts with the protein is also important for ring structures. In addition, part of the energy of complexation is spent on the

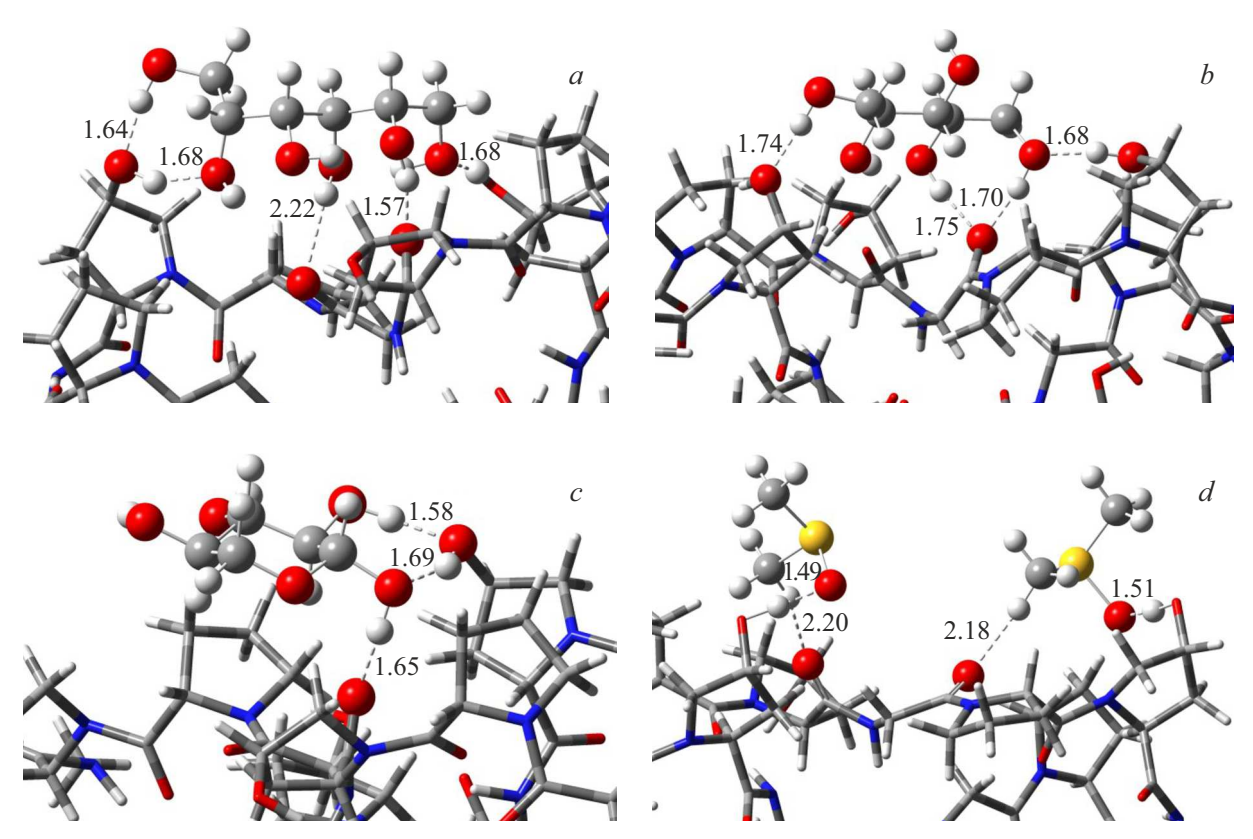


Figure 5. Fragments of molecular models of collagen peptide complexes $((GPH)_3)_2$ with molecules of sorbitol (a), xylitol (b), D-xylose (c) and DMSO (d), optimized by the HF/STO-3G method. The dashed lines show intermolecular hydrogen bonds. The numbers in the figure indicate the lengths of hydrogen bonds in angstroms.

structural change of the molecular pocket. We used the methods of quantum chemistry to take these factors into account.

A striking representative of the OCA with a minimum number of classical hydrogen bonds and a maximum interaction energy is DMSO. When interacting with collagen, DMSO is a proton acceptor, so it forms hydrogen bonds only with hydroxyproline, which has structurally accessible hydroxyl groups. Initially, only one DMSO molecule was used in modeling the interaction (the complex with the left side of the molecular pocket (Fig. 5, d)). With one classical hydrogen bond, a very high interaction energy was obtained — more than that of sorbitol with five hydrogen bonds (Table 2).

Despite this, the OCE of DMSO is so large that there was no correlation of parameters, as in other OCA. The DMSO molecule is the smallest in size among the studied OCA and occupied only one part of the molecular pocket. It was suggested that the interaction with two DMSO molecules, rather than one, should be considered. After studying the results of molecular dynamics, we found a configuration variant where the independent interaction of two DMSO molecules with one molecular pocket is visible (Fig. 4, b). By adding a second molecule and occupying the second part of the molecular pocket, an additional 91 kJ/mol was

obtained to the interaction energy. And only in this case, as can be seen from Fig. 7, there is a good correlation of the parameters. When constructing the correlation relationship, previously obtained data for other OCA were also used.

The effect of the formation of nonclassical hydrogen bonds with hydrogen atoms of methyl groups was considered earlier in Ref. [57], which leads to the formation of dimers and trimers and enhances complexes with water molecules. The atypical energy of DMSO interaction with the collagen peptide led to additional studies of intermolecular interaction using the wB97XD [58] functional, which was specially developed for the analysis of nonvalent interactions. In this case, the extended basis set 6-311+G(3d,p) was used to eliminate the error associated with the limited basis STO-3G and, accordingly, with the interpretation of the results.

Since both functional groups to which DMSO molecules attach belong to the same peptide chain, we cut out this part and examined the GPH-DMSO complex, the structure of which is shown in Fig. 8, a. We examined the complex GPH-H₂O to determine how DMSO competes with water molecules strongly bound to collagen (Fig. 8, b).

As can be seen from Fig. 8, a, when the DMSO molecule interacts with the peptide chain, five hydrogen bonds are formed: one classical between the hydroxyl

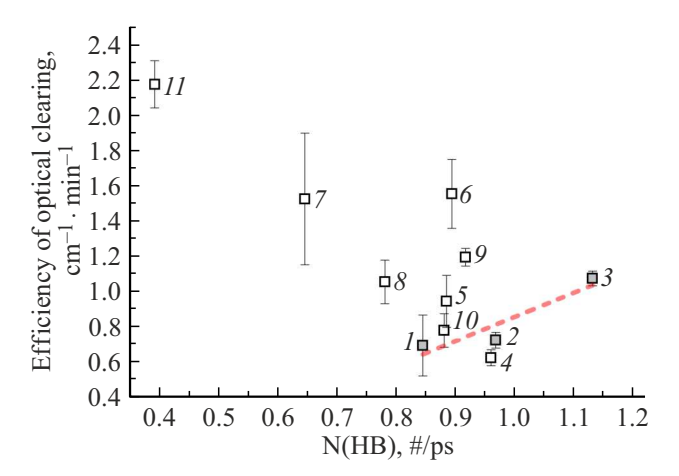


Figure 6. Dependence of the OCE value of human skin *in vivo* on the number of hydrogen bonds between clearing agents and a fragment of collagen peptide $((GPH)_3)_2$. The numbers 1-11 denote various types of clearing agents [36,37]: 1—glycerin, 2—xylitol, 3—sorbitol, 4—xylose, 5—ribose, 6—glucose, 7—fructose, 8—sucrose, 9—glucosamine, 10—yogexol, 11—DMSO. The linear approximation for the first three agents having the same linear structure is marked with a dashed line.

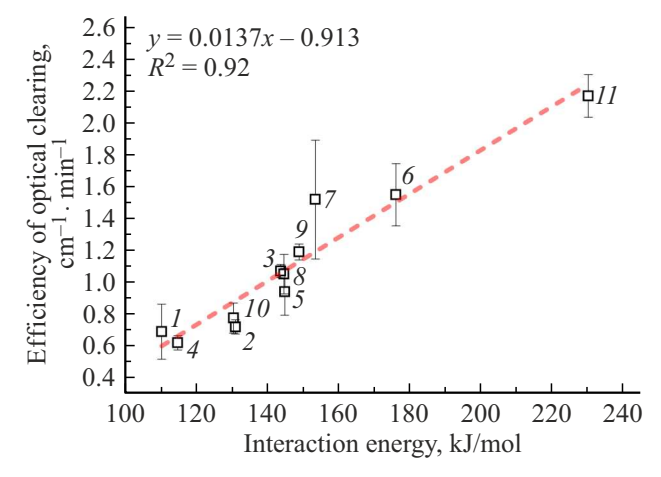


Figure 7. Dependence of the OCE value of human skin *in vivo* on the energy of intermolecular interaction between clearing agents and a fragment of collagen peptide((GPH)₃)₂. The numbers indicate various types of OCA [36,37]: 1—glycerin, 2—xylitol, 3—sorbitol, 4—xylose, 5—ribose, 6—glucose, 7—fructose, 8—sucrose, 9—glucosamine, 10—yogexole, 11—DMSO. The linear approximation is marked with a dashed line and expressed as an equation.

group of hydroxyproline and the sulfoxide group and four nonclassical — two between the oxygen of the hydroxyl group and the hydrogens of both methyl groups and two between the carbonyl group of glycine and hydrogens of another methyl group. Classical hydrogen bonds are understood as bonds formed between hydrogen atoms of hydroxyl groups and oxygen atoms of hydroxyl and carbonyl groups, and nonclassical — with the participation of hydrogens of methyl groups. The intermolecular interaction

energies were calculated taking into account the Basis Set Superposition Error (BSSE) [59]. We calculated the enthalpy of association of six complexes (Fig. 8, a-f) and a water dimer (Fig. 8, g) for temperatures of $T=0\,\mathrm{K}$ and $T=310.15\,\mathrm{K}$ by the formula

$$\Delta H_T^0 = \Delta E + \Delta ZPE + BSSE + \Delta H_{\text{term}}, \tag{6}$$

where ΔE is the difference of total electronic energies of the complex and monomers, ΔZPE is the difference of zero vibrational energies, BSSE is the superposition error, ΔH_{term} is the thermodynamic correction, as well as the equilibrium constant K_T according to the formula

$$K_T = \exp\left(-\frac{\Delta G^0}{RT}\right),\tag{7}$$

where ΔG^0 is the Gibbs free energy change, R is the gas constant, T is the temperature. The numerical values of these parameters are given in Table 3.

The table shows that, despite the higher level of theory (compared to HF/STO-3G, which clearly overestimates the electrostatic interaction), the interaction energy turned out to be quite large anyway. Hydroxyproline-DMSO complexes (Fig. 8, c) and DMSO monohydrate (Fig. 8, e) were considered to assess the contribution to the interaction energy of nonclassical hydrogen bonding. Upon formation of a complex with GPH, two more nonclassical hydrogen bonds with hydrogens of another methyl group of DMSO appear. In this case, the electron density distribution changes slightly, which affects the strengthening of the classical hydrogen bond — the length of bond O1...H2 decreases by 0.2 Å. As a result, the formation of two nonclassical hydrogen bonds and the strengthening of the classical one leads to the difference in the enthalpy of association at $T = 310.15 \,\mathrm{K}$ being 19.7 kJ/mol. Additionally, to evaluate the contribution of pure nonclassical hydrogen bonds, the DMSO monohydrate formed only with the help of two nonclassical hydrogen bonds was calculated; the structure of the monohydrate is shown in Fig. 8, d. Table 3 shows that the enthalpy of association is 10.5 kJ/mol, which is comparable in order of magnitude to the dimerization energy of water. As a first approximation, we assume that this contribution of the two nonclassical bonds is half of the enthalpy difference when comparing complexes of GPH...,DMSO and hydroxyproline...DMSO. Based on this, the contribution from the four bonds will be on the order of 20 kJ, which is equal to a third of the total enthalpy of the association. Thus, it can be concluded that the nonclassical hydrogen bond makes a significant contribution to the enthalpy of association of DMSO with collagen. It follows from the values of the equilibrium constants that GPH complexes with DMSO and H₂O molecules are very stable.

Since the dehydration process plays an important role in the optical clearing of biological tissues, it was interesting to build the first hydrate shell of the DMSO molecule. The structure of the complex is shown in Fig. 8, *e*. For

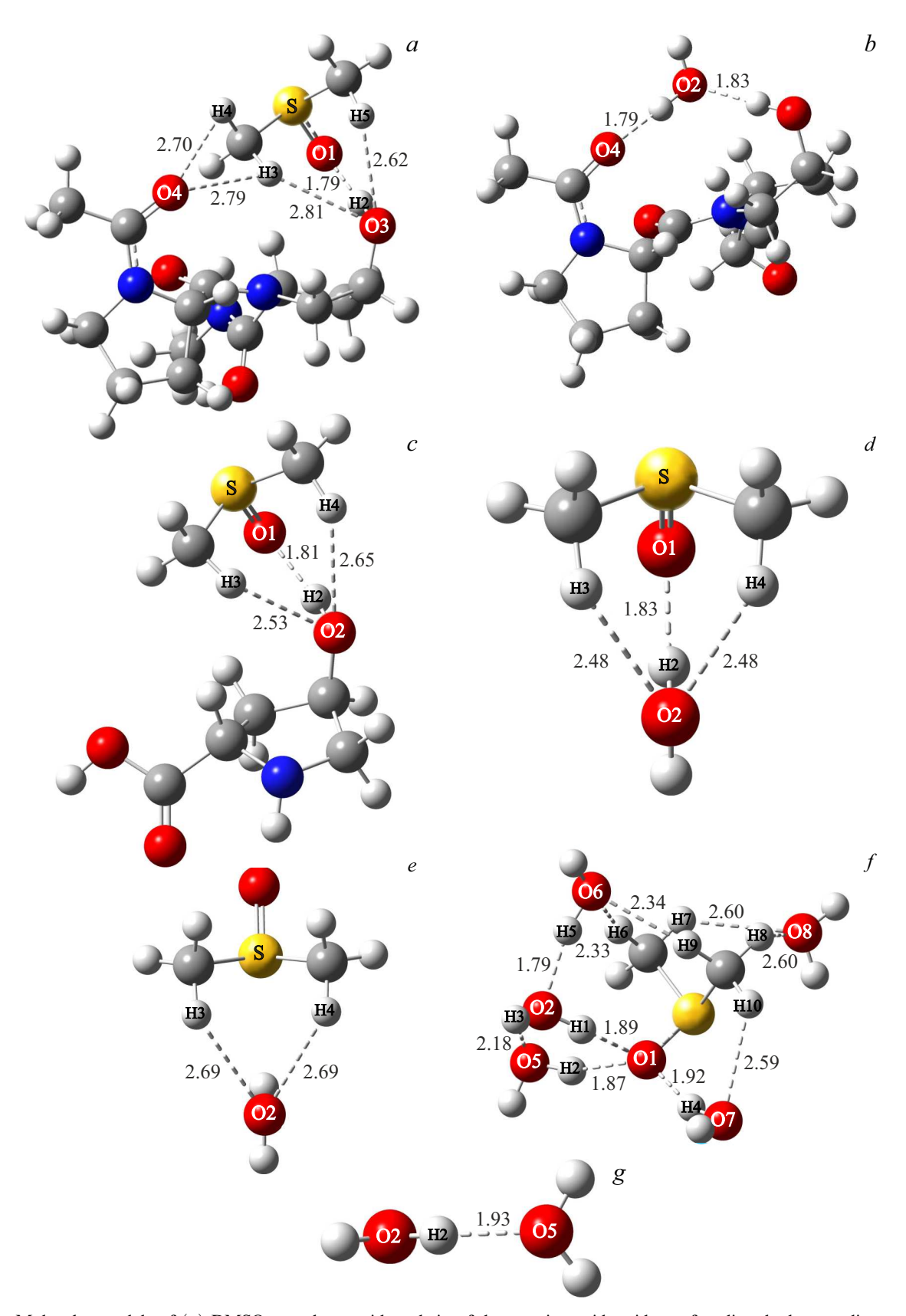


Figure 8. Molecular models of (a) DMSO complexes with a chain of three amino acid residues of proline, hydroxyproline and glycine (GPH), (b) GPH... H_2O , (c) hydroxyproline...DMSO, (d) DMSO... H_2O , (e) DMSO... H_2O , (f) DMSO... SH_2O , (g) H_2O ... H_2O , calculated using the wB97XD/6-311G+(3d,p) method. The dashed lines show hydrogen bonds. The numbers in the figure indicate the lengths of hydrogen bonds in angstroms.

Intermolecular complex	BSSE	ΔZPE	ΔE	ΔH_0^0	$\Delta H_{310.15}^{0}$	$K_{310.15}$
GPHDMSO	4.0	6.0	-74.4	-64.5	-63.4	1.652 · 102
GPHH ₂ O	3.5	9.6	-67.1	-52.1	-55.2	1.399 · 102
HydroxyprolineDMSO	2.3	6.1	-52.1	-43.7	-43.7	$7.9 \cdot 10^{-1}$
$H_2O \dots H_2O$	1.7	9.6	-23.0	-11.7	-14.1	$5.5 \cdot 10^{-3}$
$DMSOH_2O$	2.0	9.6	-43.2	-31.7	-33.7	$1.6\cdot 10^{-1}$
DMSOH ₂ O1	1.3	5.4	-17.9	-11.2	-10.5	$4.7 \cdot 10^{-4}$
DMSO5H ₂ O	11.82	41.3	-172.1	-119.0	_	_

Table 3. Thermodynamic parameters of intermolecular complexes in units of kJ/mol and equilibrium constants calculated using the BSSE method wB97XD/6-311+G(3d,p)

Note. 1 DMSO monohydrate with nonclassical hydrogen bonds.

comparative analysis, a DMSO complex with a water molecule was also built (Fig. 8, d).

According to the simulation, the first hydrate shell of DMSO consists of five water molecules. The addition of the sixth molecule to any structural position leads to the formation of a bridge from a water molecule that is no longer directly bound to the DMSO molecule and belongs to the second hydrate shell. Taking into account nonclassical hydrogen bonds and considering that two hydrogen bonds between three water molecules account for a maximum of 30 kJ/mol, on average, about 17.8 kJ/mol is spent on retaining one water molecule, which is more than the enthalpy of dimerization of water. When one water molecule binds (Fig. 8, d), three hydrogen bonds are formed — one classical and two nonclassical. The enthalpy of association in this case is approximately 2.4 times greater than that of the water dimer. It follows from the analysis that, when interacting with collagen, DMSO is in great competition even with strongly bound water molecules that form two hydrogen bonds with collagen. Thus, DMSO, on the one hand, binds free water very well, and on the other hand, when interacting with collagen, it competitively occupies the space previously occupied by water molecules. This process can lead to disruption of the hydrogen bonding network and reversible dissociation of collagen, which also affects the process of optical clearing of biological tissues.

An indirect confirmation of this hypothesis is the effect of OCA on the volume of collagen peptide. In this regard, it was interesting to compare the effect of the DMSO molecule on the structure of collagen with the most popular immersion agent glycerin and the yogexole molecule, which is one of the largest molecules used as an immersion agent, not including repeating structures such as polyethylene glycol (PEG).

Fig. 4, c, d shows the spatial distribution of DMSO molecules around the collagen peptide 5GPH₁₂)₃ at the beginning of observation (c) and after one nanosecond (d). As can be seen from the figure, the interaction of DMSO

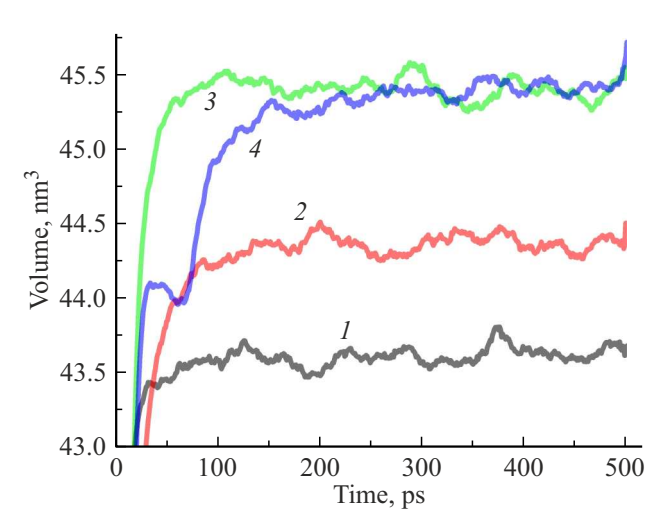


Figure 9. Dependence of changes in the volume of collagen peptide on the time of exposure to OCA: without OCA (pure water) -1, 60% aqueous solutions of DMSO -2, glycerin -3and yogexol — 4.

with collagen increases its volume compared to water. This is due to the fact that the size of the OCA molecules is larger than the water molecules, and this leads to an increase in volume. At the same time, the network of hydrogen bonds is also disrupted. This factor also affects the change in the refractive index of collagen and the probability of reversible dissociation. A comparative graph of changes in the volume of collagen peptide under the action of some OCA of different molecular structures is shown in Fig. 9.

It can be seen from Fig. 9 that in this case, the change in the volume of the collagen peptide is most influenced by glycerol and yogexol molecules. These molecules have markedly different structural sizes. Presumably, this may be attributable to both the different sizes of the first hydrate shells and the formation of stable self-associates, which creates an additional "effective" molecular size. Glycerol

² BSSE was calculated using the partial BSSE method, when the values calculated for each water molecule are added together.

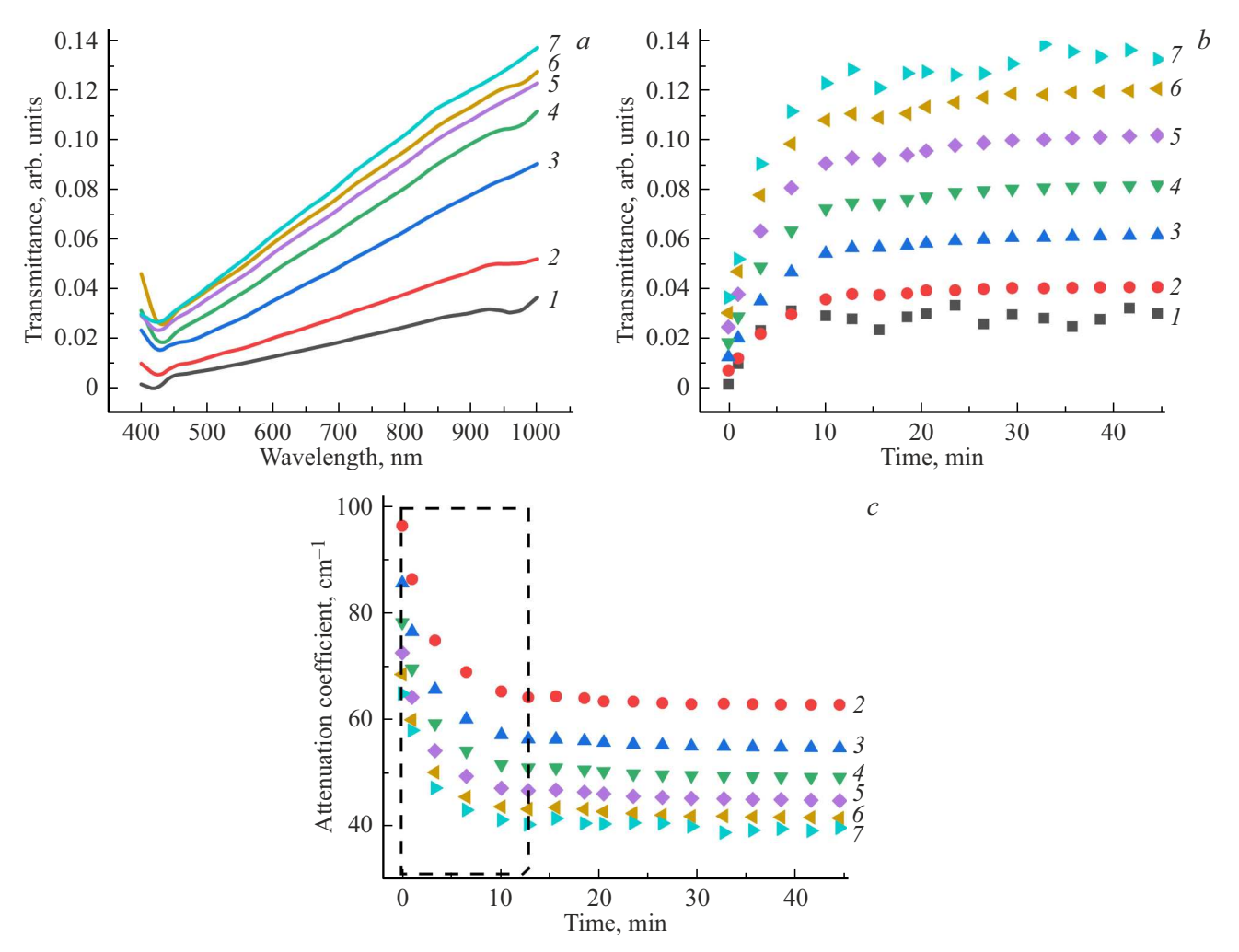


Figure 10. Typical change in the coefficient of collimated transmittance of a skin sample under the action of DMSO, depending on (a) wavelengths (the numbers indicate the time points at which the measurement was performed: I = 0, 2 = 1, 3 = 3, 4 = 6, 5 = 10, 6 = 20, 7 = 45 min). The dependences of the coefficient of collimated transmittance (b) and the attenuation coefficient (c) on time (the numbers indicate the wavelengths: I = 400, I = 200, I = 300, I =

has much more of these structural possibilities than yogexol. Additional study is required to provide an unambiguous explanation of the results of this simulation.

A very important parameter that affects the experimental value of the optical clearing efficiency is the diffusion rate of the immersion agent into the skin. This is attributable to the fact that the OCE parameter includes the time it takes for the scattering coefficient to decrease. The faster the immersion agent penetrates into the tissue, the faster processes such as dehydration and interaction with collagen begin to work. Fig. 10 shows typical spectral and temporal dependences of the coefficient of collimated skin transmittance under the action of DMSO and the kinetics of the attenuation coefficient. It is clearly seen that the collimated transmittance of intact skin ranges from approximately 0 to 3.5 % in the range from 400 to 1000 nm, respectively (Fig. 10, f). After 45 min of exposure to DMSO, the coefficient of collimated transmittance increases by \sim 18

times (400 nm) and by 4 times (1000 nm). Since significant signal fluctuations were observed at a wavelength of 400 nm (curve I in Fig. 10, b), kinetic curves at wavelengths of 500 (2), 600 (3), 700 (4), 800 (5), 900 (6) and 1000 (7) nm were used to estimate the OCE and the effective diffusion constant, where the time dependences of the coefficient are quite smooth.

It is known that the effective diffusion coefficient is determined by the exchange flow of hyperosmotic substance into the tissue and water from the interstitial space. The obtained value of the effective diffusion coefficient of DMSO (average \pm standard error of the average) in the skin was $(4.1\pm3.1)\cdot 10^{-6}~\rm cm^2/s$, weighted average — $(3.95\pm0.04)\cdot 10^{-6}~\rm cm^2/s$. This value exceeds the values obtained for OCA in the skin, such as PEG-300 (1.83), PEG-400 (1.7), 85%- glycerol solution (1.81) having similar refractive index values, but significantly higher viscosity values: 110, 135 and 109 mPa·s, while

the viscosity of DMSO is only 1.99 mPa·s. [6]. The closest value obtained corresponds to the value of the effective diffusion coefficient of 100 % glycerol in the skin: $(3.23\pm2.21)\cdot10^{-6})$ cm²/s [60]. However, the viscosity of dehydrated glycerol is 1410 MPacots. Thus, in the case of glycerin, there is a predominant diffusion of water into the surrounding OCA solution and significant dehydration of the tissue.

The OCE value obtained from the kinetics of the spectra of collimated skin transmittance under the action of DMSO averaged $2.1 \pm 0.5 \, \text{cm}^{-1} \text{min}^{-1}$, which is in good agreement with the results of the OCE estimation using OCT, presented in Table 2.

It should be noted that when modeling, we do not take into account the rate of OCA diffusion into the skin. We model only the post-diffusion part of optical illumination, i.e. the process of interaction of OCA with collagen. Despite this, we still have a good correlation between the energy of intermolecular interaction and OCE, which allows using this parameter for the theoretical prediction of the properties of OCA.

Conclusion

Based on experimental in vivo data, the OCE of human skin was determined for aqueous solutions of sorbitol, xylitol, D-xylose and pure DMSO. The effective diffusion coefficient of DMSO was calculated based on ex vivo data for the collimated transmittance of rat skin samples, which turned out to be relatively high and, having a low viscosity, DMSO quickly penetrates the skin and begins to interact with collagen, which increases the value of OCE. The complex molecular modeling of the interaction of the considered OCA with the collagen peptide showed that there is a correlation between the energy of intermolecular interaction and the OCE of human skin, which allows this parameter to be used for predictive purposes. For the DMSO molecule, such a correlation exists only if the interaction of two molecules with the molecular pocket of the collagen peptide is considered at once. The absence of hydroxyl groups and the presence of two hydrophobic methyl groups does not prevent the DMSO molecule from forming noticeable nonclassical hydrogen bonds with them and from competing highly with water molecules when interacting with collagen. During the formation of the first hydrate shell of DMSO, the average interaction energy per water molecule is noticeably higher than the energy of the formation of a water dimer, which indicates the possibility of effectively retaining free water around itself. It is assumed that changes in the volume of collagen during interaction, in addition to the size of the OCA molecules themselves, are influenced by the size of the first hydrate shell and the ability to create stable self-associations.

Funding

The work has been funded by the grant (N_2 23-14-00287) from the Russian Science Foundation.

Conflict of interest

The authors declare that they have no conflict of interest.

References

- [1] V.V. Tuchin. *Tissue optics: light scattering methods and instruments for medical diagnostics*, 3rd ed. (PM 254, SPIE Press, Bellingham, WA, 2015). DOI: 10.1117/3.1003040
- H. Jonasson, I. Fredriksson, S. Bergstrand, C.J. Östgren,
 M. Larsson, T. Strömberg. J. Biomed. Opt., 23 (12), 121608
 (2018). DOI: 10.1117/1.JBO.23.12.121608
- [3] Handbook of tissue optical clearing: new prospects in optical imaging, ed. by V.V. Tuchin, D. Zhu, E.A. Genina (Taylor & Francis Group LLC, CRC Press, Boca Raton, FL, 2022). DOI: 10.1201/9781003025252
- [4] J.M. Hirshburg. Chemical agent induced reduction of skin light scattering: doctoral dissertation (Texas A & M University, 2009).
- [5] D. Zhu, K.V. Larin, Q. Luo, V.V. Tuchin. Laser Photonics Rev., 7 (5), 732 (2013). DOI: 10.1002/lpor.201200056
- [6] A.N. Bashkatov, K.V. Berezin, K.N. Dvoretskiy, M.L. Chernavina, E.A. Genina, V.D. Genin, V.I. Kochubey, E.N. Lazareva, A.B. Pravdin, M.E. Shvachkina, P.A. Timoshina, D.K. Tuchina, D.D. Yakovlev, D.A. Yakovlev, I.Yu. Yanina, O.S. Zhernovaya, V.V. Tuchin. J. Biomed. Opt., 23 (9), 091416 (2018). DOI: 10.1117/1.JBO.23.9.091416
- [7] L. Oliveira, V.V. Tuchin. The optical clearing method: a new tool for clinical practice and biomedical engineering (Springer Nature Switzerland AG, Basel, 2019).
 DOI: 10.1007/978-3-030-33055-2
- [8] I. Costantini, R. Cicchi, L. Silvestri, F. Vanzi, F.S. Pavone. Biomedical Optics Express, 10 (10), 5251 (2019). DOI: 10.1364/boe.10.005251
- [9] P. Matryba, L. Kaczmarek, J. Gołąb. Laser Photonics Rev., 13 (8), 1800292 (2019). DOI: 10.1002/lpor.201800292
- [10] T. Yu, J. Zhu, D. Li, D. Zhu. iScience, 24 (3), 102178 (2021). DOI: 10.1016/j.isci.2021.102178
- [11] I.S. Martins, H.F. Silva, E.N. Lazareva, N.V. Chernomyrdin, K.I. Zaytsev, L.M. Oliveira, V.V. Tuchin. Biomedical Optics Express, 14 (1), 249 (2023). DOI: 10.1364/BOE.479320
- [12] E.C. Cheshire, R.D.G. Malcomson, S. Joseph, A. Adnan, D. Adlam, G.N. Rutty. Int. J. Legal Med., 131, 1377 (2017). DOI: 10.1007/s00414-017-1570-1
- [13] T. Yu, J. Zhu, Y. Li, Y. Ma, J. Wang, X. Cheng, S. Jin, Q. Sun, X. Li, H. Gong, Q. Luo, F. Xu, S. Zhao, D. Zhu. Sci. Rep., 8 (1), 1964 (2018). DOI: 10.1038/s41598-018-20306-3
- J. Musakhanian, D.W. Osborne, J-D. Rodier. AAPS Pharm-SciTech, 25 (7), 201 (2024).
 DOI: 10.1208/s12249-024-02886-8
- [15] E.A. Genina, A.N. Bashkatov, E.A. Kolesnikova, M.V. Basko, G.S. Terentyuk, V.V. Tuchin. J. Biomed. Optics, 19 (2), 021109 (2013). DOI: 10.1117/1.JBO.19.2.021109
- [16] B. Kumar, S.K. Jain, S.K. Prajapati. Intern. J. Drug Delivery, 3 (1), 93 (2011). DOI: 10.5138/ijdd.2010.0975.0215.03057

- [17] S.M. Zaytsev, Yu.I. Svenskaya, E.V. Lengert, G.S. Terentyuk, A.N. Bashkatov, V.V. Tuchin, E.A. Genina. J. Biophotonics, 13 (4), e201960020 (2020). DOI: 10.1002/jbio.201960020
- [18] S. Karma, J. Homan, C. Stoianovici, B. Choi. J. Innovative Optical Health Sciences, (3) 3, 153 (2010). DOI: 10.1142/S1793545810001015
- [19] A.K. Bui, R.A. McClure, J. Chang, C. Stoianovici, J. Hirshburg, A.T. Yeh, B. Choi. Lasers in Surgery and Medicine, 41 (2), 142 (2009). DOI: 10.1002/lsm.20742
- [20] X. Wen, S.L. Jacques, V.V. Tuchin, D. Zhu. J. Biomed. Opt., 17 (6), 066022 (2012). DOI: 10.1117/1.JBO.17.6.066022
- [21] A.N. Bashkatov, E.A. Genina, V.V. Tuchin. Handbook of optical sensing of glucose in biological fluids and tissues, ed. by V.V. Tuchin (Taylor & Francis Group LLC, CRC Press, 2009), ch. 21. DOI: 10.1201/9781584889755
- [22] K.V. Larin, V.V. Tuchin. Quantum Electronics, 38 (6), 551 (2008). DOI: 10.1070/QE2008v038n06ABEH013850.
- [23] D.K. Tuchina, R. Shi, A.N. Bashkatov, E.A. Genina, D. Zhu, Q. Luo, V.V. Tuchin. J. Biophotonics, 8 (4), 332 (2015). DOI: 10.1002/jbio.201400138
- [24] V. Hovhannisyan, P.-S. Hu, S.-J. Chen, C.-S. Kim, C.-Y. Dong.
 J. Biomed. Opt., 18 (4), 046004 (2013).
 DOI: 10.1117/1.JBO.18.4.046004
- [25] A.Yu. Sdobnov, M.E. Darvin, E.A. Genina, A.N. Bashkatov, J. Lademann, V.V. Tuchin. Spectrochimica Acta Part A: Molecular and Biomolecular Spectroscopy, 197, 216 (2018). DOI: 10.1016/j.saa.2018.01.085
- [26] A.T. Yeh, B. Choi, J.S. Nelson, B.J. Tromberg. J. Investigative Dermatology, 121 (6), 1332 (2003). DOI: 10.1046/j.1523-1747.2003.12634.x
- [27] Z. Ou, Yi-Sh. Duh, N.J. Rommelfanger, C.H.C. Keck, Sh. Jiang, K. Brinson Jr., S. Zhao, E.L. Schmidt, X. Wu, F. Yang, B. Cai, H. Cui, W. Qi, Sh. Wu, A. Tantry, R. Roth, J. Ding, X. Chen, J.A Kaltschmidt, M.L. Brongersma, G. Hong. Science, 385 (6713), eadm6869 (2024). DOI: 10.1126/science.adm686
- [28] V.V. Tuchin, D.M. Zhestkov, A.N. Bashkatov, E.A. Genina. Optics Express, 12 (13), 2966 (2004). DOI: 10.1364/OPEX.12.002966
- [29] V.V. Tuchin. Optical clearing of tissues and blood (PM 154, SPIE Press, Bellingham, WA, 2005). DOI: 10.1117/3.637760
- [30] O. Sydoruk, O. Zhernovaya, V. Tuchin, A. Douplik. J. Biomed. Opt., 17 (11), 115002-1-6 (2012).
 DOI: 10.1117/1.JBO.17.11.115002
- [31] O. Zhernovaya, V.V. Tuchin, M.J. Leahy. J. Biomed. Opt., 18 (2), 026014-1-8 (2013). DOI: 10.1117/1.JBO.18.2.026014
- [32] O.S. Zhernovaya, E.A. Genina, V.V. Tuchin, A.N. Bashkatov. Handbook of tissue optical clearing: new prospects in optical imaging, ed. by V.V. Tuchin, D. Zhu, E.A. Genina (Taylor & Francis Group LLC, CRC Press, Boca Raton, FL, 2022), p. 383–392. DOI: 10.1201/9781003025252
- [33] T. Yu, X. Wen, V.V. Tuchin, Q. Luo, D. Zhu. J. Biomed. Opt., **16** (9), 095002 (2011). DOI: 10.1117/1.3621515
- [34] X. Wen, Z. Mao, Z. Han, V.V. Tuchin, D. Zhu. J. Biophotonics, **3** (1–2), 44 (2010). DOI: 10.1002/jbio.200910080
- [35] A.Yu. Sdobnov, M.E. Darvin, J. Schleusener, J. Lademann, V.V. Tuchin. J. Biophotonics, 12 (5), e201800283 (2019). DOI: 10.1002/jbio.201800283
- [36] K.V. Berezin, E.V. Grabarchuk, A.M. Lichter, K.N. Dvoretski, V.V. Tuchin. J. Biophotonics, 17 (2), e202300354 (2024). DOI: 10.1002/jbio.202300354

- [37] K.V. Berezin, E.V. Grabarchuk, A.M. Lichter, K.N. Dvoretski, Yu.I. Surkov, V.V. Tuchin. Technical Physics, 69 (3), 485 (2024). DOI: 10.21883/0000000000.
- [38] C.C.J. Roothaan. Rev. Modern Phys., 23 (2), 69 (1951).DOI: 10.1103/RevModPhys.23.69
- [39] R. Goldberg, B. Lang, B. Coxon, S. Decker. J. Chem. Thermodynamics, 15 (2), 2 (2012). DOI: 10.1016/j.jct.2011.07.004
- [40] D.J. Faber, F.J. van der Meer, M.C.G. Aalders, T.G. van Leeuwen. Opt. Express, 12 (19), 4353 (2004). DOI: 10.1364/OPEX.12.004353
- [41] P. Lee, W. Gao, X. Zhang. Appl. Opt., 49 (18), 3538 (2010). DOI: 10.1364/AO.49.003538
- [42] E.A. Genina, A.N. Bashkatov, E.A. Kolesnikova, M.V. Basko, G.S. Terentyuk, V.V. Tuchin. J. Biomed. Opt., 19 (2), 021109 (2014). DOI: 10.1117/1.JBO.19.2.021109
- [43] R.K. Wang, V.V. Tuchin. Handbook of coherent-domain optical methods, biomedical diagnostics, environmental monitoring, and material science, 2nd ed., ed. by V.V. Tuchin (Springer-Verlag, Berlin, Heidelberg, N.Y., 2013), vol. 2, p. 665. DOI: 10.1007/978-1-4614-5176-1
- [44] E.A. Genina, N.S. Ksenofontova, A.N. Bashkatov, G.S. Terentyuk, V.V. Tuchin. Quantum Electronics, 47 (6), 561 (2017). DOI: 10.1070/QEL16378.
- [45] K. Okuyama, K. Miyama, K. Mizuno, H.P. Bachinger. Biopolymers, 97 (8), 607 (2012). DOI: 10.1002/bip.22048
- [46] W.D. Cornell, P. Cieplak, C.I. Bayly, I.R. Gould, K.M.Jr. Merz, D.M. Ferguson, D.C. Spellmeyer, T. Fox, J.W. Caldwell, P.A. Kollman. J. Am. Chem. Soc., 117 (19), 5179 (1995). DOI: 10.1021/ja00124a002
- [47] A.D. Becke. J. Chem. Phys., 98 (7), 5648 (1993). DOI: 10.1063/1.464913
- [48] C. Lee, W. Yang, R.G. Parr. Phys. Rev. B, 37 (2), 785 (1988). DOI: 10.1103/PhysRevB.37.785
- [49] M.J. Frisch, G.W. Trucks, H.B. Schlegel et al. *Gaussian09*, revision A.02 (Gaussian Inc, Pittsburgh PA, 2009).
- [50] D. Van der Spoel, E. Lindahl, B. Hess, G. Groenhof, E.A. Mark, H.J.C. Berendsen. J. Comput. Chem., 26 (16), 1701 (2005). DOI: 10.1002/jcc.20291
- [51] Y. Duan, C. Wu, S. Chowdhury, M.C. Lee, G. Xiong, W. Zhang, R. Yang, P. Cieplak, R. Luo, T. Lee, J. Caldwell, J. Wang, P. Kollman. J. Comp. Chem., 24 (16), 1999 (2003). DOI: 10.1002/jcc.10349
- [52] H.J.C. Berendsen, J.P.M. Postma, W.F. van Gunsteren, A. Di-Nola, J.R. Haak. J. Chem. Phys., 81 (8), 3884 (1984). DOI: 10.1063/1.448118
- [53] W. Humphrey, A. Dalke, K. Schulten. J. Mol. Graph., 14 (1), 33 (1996). DOI: 10.1016/0263-7855(96)00018-5
- [54] H.D. Loof, L. Nilsson, R. Rigler. J. Am. Chem. Soc., 114 (11), 4028 (1992). DOI: 0.1021/ja00037a002
- [55] K.V. Berezin, K.N. Dvoretski, M.L. Chernavina, A.M. Likhter, V.V. Smirnov, I.T. Shagautdinova, E.M. Antonova, E.Yu. Stepanovich, E.A. Dzhalmuhambetova, V.V. Tuchin. J. Mol. Modeling., 24 (2), 45 (2018). DOI: 10.1007/s00894-018-3584-0
- [56] Y. Duan, C. Wu, S. Chowdhury, M.C. Lee, G. Xiong, W. Zhang, R. Yang, P. Cieplak, R. Luo, T. Lee, J. Caldwell, J. Wang, P. Kollman. J. Comp. Chem., 24 (16), 1999 (2003). DOI: 10.1002/jcc.10349
- [57] A. Jumabaev, H. Hushvaktov, B. Khudaykulov, A. Absanov, M. Onuk, I. Doroshenko, L. Bulavin. Ukr. J. Phys., 68 (6), 375 (2023). DOI: 10.15407/ujpe68.6.375

- [58] J.-D. Chai, M. Head-Gordon. J. Chem. Phys., 128 (8), 084106 (2008). DOI: 10.1063/1.2834918
- [59] S. Simon, M. Duran, J.J. Dannenberg. J. Chem. Phys., 105 (24), 11024–11031 (1996). DOI: 10.1063/1.472902
- [60] V.D. Genin, D.K. Tuchina, A.J. Sadeq, E.A. Genina, V.V. Tuchin, A.N. Bashkatov. J. Biomed. Photonics & Engineering, 2 (1), 010303 (2016). DOI: 10.18287/JBPE16.02.010303

Translated by A.Akhtyamov